the general science journal

The Gyro-Gravitational Spin Vector Torque Dynamics of Main Belt Asteroids in relationship with their Tilt and their Orbital Inclination.

described by using
the Maxwell Analogy for gravitation.

T. De Mees - thierrydm @ pandora.be

Abstract

Several observational studies of the main belt asteroids showed a direct link between the evolution of the spin vectors and the inclination of their orbit. A study wherein the evolution of 25 main belt asteroids and 125 synthetic objects was computed over 1Myr (E. Skoglöv, A. Erikson, 2002) clearly quantified this link. Verification of these results with the observation of 73 asteroids confirmed the results. Non-gravitational (YORP-/Yarkovsky-) torques are not considered here. Following observational conclusions have been made by E. Skoglöv and A. Erikson:

- the spin oscillations' amplitude increases with increasing orbital inclination of the asteroid.
- the largest spin oscillations' amplitudes are found if the initial spin vector lays in the orbital plane.
- the spin obliquity differences are generally insensitive to the shape, composition and spin rate of the asteroids.
- there is a significant majority of asteroids with a prograde spin vector compared to retrograde ones.
- the spin vectors of prograde asteroids are more chaotic than the spin vectors of retrograde asteroids.
- there are very few asteroids having a spin vector that lays in the vicinity of the orbital plane.
- the heliocentric distance is relevant for the spin vector behaviour.

In this paper it was found that the gyro-gravitation theory, which is the closest Euclid theory to the General Relativity Theory of Einstein, complies very well with these observations.
We find that the asteroid's tilt swings continuously during a full orbit. The theoretical values of the cyclic tilt variations are calculated.

Keywords: Main Belt Asteroids – gravitation – gyrotation – prograde – retrograde – orbit – precession – nutation.
Method: Analytical.

1. Orbital data of the main belt asteroids, by E. Skoglöv and A. Erikson.

In our solar system, the orbital evolution of the main belt asteroids is primarily influenced by Saturn and Jupiter. The orbital perturbations are ordinarily periodic in the sense that they vary between certain limits. The spin vectors of asteroids can be influenced by nearby passing planets, by collisions, but there has also been observed a mechanism due to the asteroids' orbital evolution.
When I discovered the papers of E. Skoglöv and A. Erikson, I became intrigued by their results. In these papers, the latter mechanism (the one related to the asteroids' orbital evolution) has been observed and reported. This means that the orbital perturbations by Saturn and Jupiter have not been studied here, but only the relationship between both the initial spin orientation and the orbital evolution, in relation with the spin vector evolution of the asteroid.

1.1. Basic data of 25 real objects.

Table 1.1 shows which 25 large asteroids have been chosen (E. Skoglöv, A. Erikson, 2002) to perform the observations.
The average semi-major axis of the orbit is given and the orbital inclinations: maximal, minimal and average.
These orbital variations, caused by Jupiter and Saturn, generate spin vector changes.
On these data, the study of E. Skoglöv and A. Erikson has been based on.

Asteroid	i_{min} (°)	i_{ave} (°)	i_{max} (°)	a_{ave} (AU)
1 Ceres	7.3	9.7	12.0	2.77
2 Pallas	26.5	33.2	38.7	2.77
5 Astraea	2.2	4.7	7.0	2.58
6 Hebe	11.6	14.4	17.2	2.43
7 Iris	3.8	6.5	9.0	2.39
9 Metis	2.3	4.9	7.2	2.39
17 Thetis	2.4	5.0	7.3	2.47
18 Melpomene	7.0	9.9	12.6	2.30
19 Fortuna	0.0	2.6	4.6	2.44
20 Massalia	0.0	2.0	3.8	2.41
23 Thalia	6.8	9.7	12.5	2.63
31 Euphrosyne	22.8	26.5	30.3	3.16
32 Pomona	3.8	6.2	8.5	2.59
39 Laetitia	7.6	9.9	12.1	2.77
41 Daphne	11.5	15.5	19.5	2.76
51 Nemausa	7.4	10.1	12.7	2.37
64 Angelina	0.1	2.6	4.5	2.68
130 Elektra	18.9	22.1	25.3	3.12
243 Ida	0.0	2.4	4.2	2.86
270 Anahita	0.5	3.6	6.3	2.20
451 Patientia	11.8	14.0	16.2	3.06
471 Papagena	10.9	13.8	16.5	2.89
694 Ekard	14.5	18.0	21.9	2.67
776 Berbericia	14.6	17.2	19.7	2.93
852 Wladilena	20.1	24.0	28.0	2.36

Table 1.1 *(source : E. Skoglöv, A. Erikson)*

The Minimum, Average, and Maximum Orbital Inclination (i_{min}, i_{ave}, and i_{max} Respectively) Together with the Average Value of the Semi-major Axis of the Orbit (a_{ave}) for the 25 Real Main Belt Asteroids

1.2. The results of the study for the 25 real objects.

In fig.1.2 has been drawn the evolution of the spin vector $X = \cos \varepsilon$, where ε is the obliquity of the spin vector, which means the tilt of the spin axis from the normal to the orbital plane, as shown in fig.1.1.

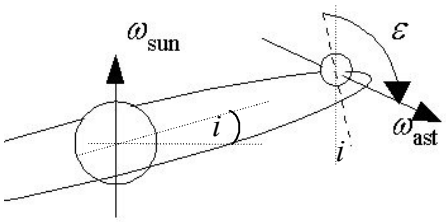

Fig. 1.1 : definition of the obliquity ε of the asteroid's spin vector and the orbital inclination i.

The ordinate of Fig. 1.2 shows the minimum and maximum values of this obliquity after a time period of 1 Myr (10^6 years).
The figure also shows the precession frequency ($p = \mathrm{d}\,\psi / \mathrm{d}\,t$) wherein ψ is the precession angle of the spin vector.

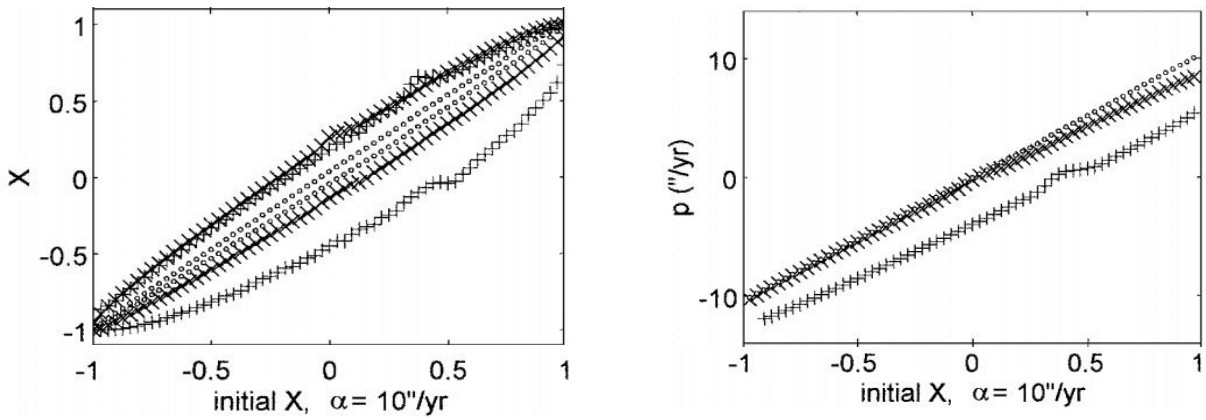

(source : E. Skoglöv, A. Erikson)

Fig. 1.2. The average precession frequency ($p = d\psi/dt$) and the minimum and maximum X values ($X = \cos \varepsilon$, where ε is the obliquity) obtained during the time period [0,1] Myr for 65 equidistant initial X values for objects having the orbital evolutions of 1 Ceres ($i_{ave} = 9.7°$, ×), 20 Massalia ($i_{ave} = 2.0°$, ○), and 694 Ekard ($i_{ave} = 18.0°$, +). The artificial precession parameter (α) is 10″/yr and the time step of the spin axis integration is 3.125 years. Note the increase in ΔX, the difference between the maximum and minimum X values, with larger orbital inclinations. The largest ΔX values are obtained for initial values close to $X = 0$.

The fig. 1.2 should be read as follows. The spin obliquity of three asteroids, Ceres with i_{ave} = 9.7°, indicated with ×, Massalia (i_{ave} = 2.0°, o) and Ekard (i_{ave} = 18.0°, +) have been plotted. The initial value $X = \cos \varepsilon$ gives the spin obliquity at the time zero, and the maximal and minimal spin obliquities X are given for each of the asteroids, after the time span of 1 Myr.
In this discussion we consider our planetary system such that the spin of the sun points upwards.
The plotted results give quite a lot of information about the change of the spin vector obliquity over the given time span. The maximal and minimal values are symmetric for Ceres and Massalia. The larger the value of the orbital inclination is, the larger is the ΔX between the maximal and minimal values of the computed spin obliquities X. The ΔX between the maximal and minimal values lays in the region of an initial value X of zero, where the initial spin vector obliquity equals to 90°, and hence is laying in the orbital plane.
According to the computation, the initial spin vectors which are perpendicular to the orbital plane of the asteroids, would almost remain unchanged. However, there is a less stable situation when the initial value X is directed upwards than when the vector is directed downwards.

The results for the asteroid Ekard are significantly different for both the maximal and the minimal values of the computed spin obliquities X , i.e. a clear tendency towards lower values. This means that the spin vectors tend to point more downwards.

1.3. Basic data of 125 synthetic objects.

Besides these 25 real objects, 125 synthetic objects have been created, based on the properties of the 25 real objects but with artificial orbital inclinations i_{ave} of 5°, 10°, 15°, 20° and 25°. An artificial precession parameter has been introduced as well, for the use of the numerical extrapolation.
I assume that E. Skoglöv and A. Erikson used the best possible numerical integration and the best possible empirical adaptations to obtain the 1 Myr extrapolation for these synthetic objects. Indeed, the exact physical process is up to now unknown, and the results must be interpreted as being entirely empirical.

1.4. The results of the study for the 125 synthetic objects.

In fig. 1.3. is computed how the behaviour of the synthetic asteroids changes with time, based on the real data of Ceres. In this case, only the delta is plotted and not the absolute values of computed spin obliquities X. The legend is : orbital inclinations of 5° (o), 10° (+), 15° (×), 20° (O) and 25° (*).
The same conclusions can be taken as with the real objects.

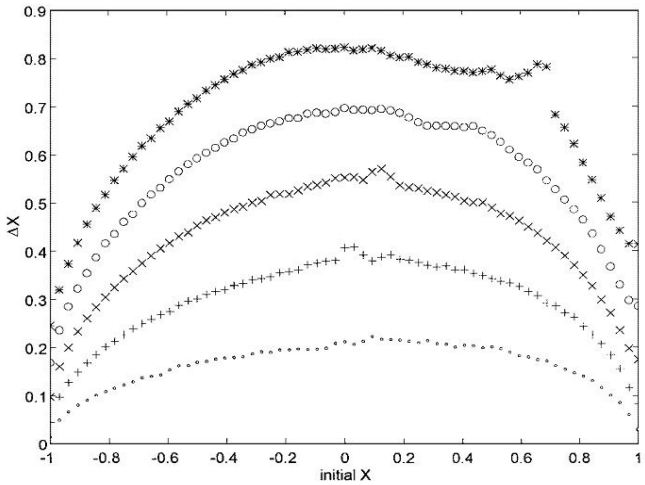

(source : E. Skoglöv, A. Erikson)

The difference between maximum and minimum X values, ΔX, for each initial step in X for five synthetic objects based on the properties of 1 Ceres, but with five different synthetic average orbital inclinations, 5° (○), 10° (+), 15° (×), 20° (○), and 25° (✳). The largest ΔX values are found for initial X values close to $X = 0$, as is also the largest increase in ΔX when the orbital inclination (i) is increased. This situation is typical for a majority of the objects studied.

Fig. 1.3

When the inclination of asteroid's orbital plane is very large, there remains a significant ΔX, even for asteroids which are perpendicular to their orbital plane, especially for those perpendicular ones that are pointed downwards.

The instability of the latter asteroids is greater than that of the former ones.

Another graphic describes how the maximal values of ΔX can be plotted in relation to the orbital inclinations of the synthetic asteroids. The results are shown in fig. 1.4. Again, we see that the larger the value of the orbital inclination, the larger the maximal ΔX becomes.
Both the 25 real objects (× , the least square method gives the lower line) and the 125 synthetic objects (o , the least square method gives the upper line) are shown.

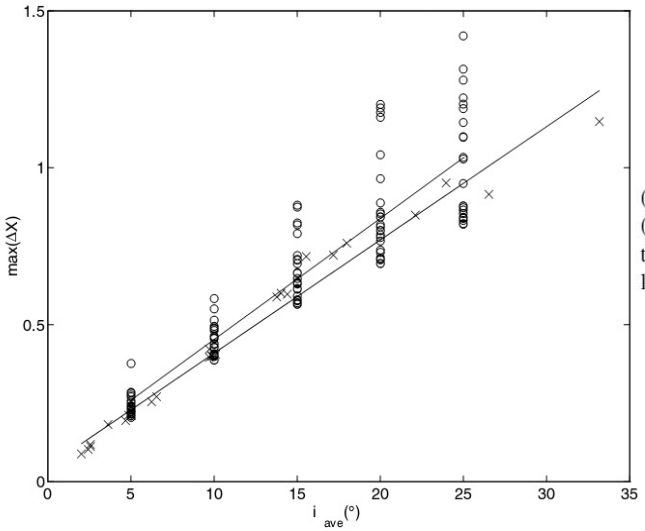

(source : E. Skoglöv, A. Erikson)

The maximum value of ΔX as a function of orbital inclination (i) for the 25 real objects (×; lower line), and for the 125 synthetic objects (○; upper line). In both cases, ΔX grows in an approximately linear way when the inclination is increased. The least-squares method has been used to adjust linear relations to the data.

Fig. 1.4

The two lines suggest a linear behaviour, but there are clear deviations. The lower end of the individual results of the 125 synthetic objects is showing a steadily slower increase of the maximal ΔX with increasing orbital inclination. Since the number of such asteroids is high, this tendency is representative.

1.5. Observational conclusions.

Out of this study, a number of quantitative and qualitative conclusions are made.

- It follows directly from the fig.1.2 , fig.1.3 and fig.1.4. that the spin oscillations' amplitude increases with an increasing orbital inclination of the asteroid.
- Out of fig.1.2 and fig.1.3, the largest spin oscillations' amplitudes are found if the initial spin vector lays in the orbital plane.
- It is found from the integration method[9] [10], that the spin obliquity differences are generally insensitive to the shape, composition and spin rate of the asteroids.
- It appears[12] that the spin vectors of prograde asteroids are more chaotic than the spin vectors of retrograde asteroids.
- Also it has been found[12] that the heliocentric distance is relevant for the spin vector behaviour.

2. The observed spin vector distribution, by A. Erikson.

2.1. The spin vector distribution of 73 asteroids of the Main Belt.

Very important data of the asteroids exist because special efforts have been made during the last decade to observe this for long time neglected subject, while much more information was collected about the planets.

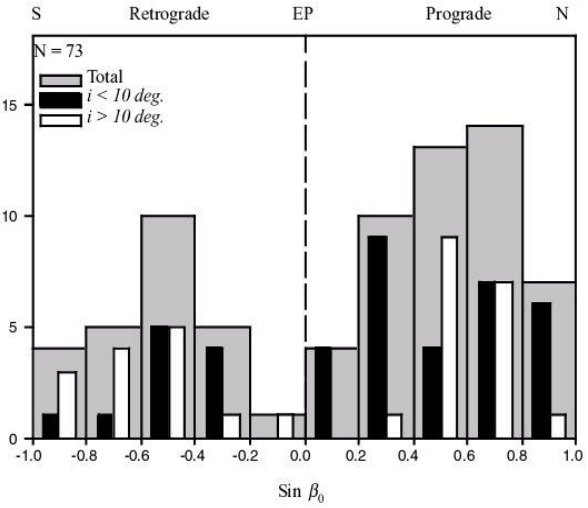

(source : A. Erikson, 2000)

The distribution of the ecliptic latitudes (β_0) of the spin vectors for 73 main belt asteroids from Erikson (2000). The included objects have been divided into two subsets with respect to their orbital inclination (i). Note the absence of asteroids with high orbital inclinations whose spin vectors are in the vicinity of the ecliptic plane (EP).

Fig. 2.1

In fig. 2.1 there have been several parameters of 73 real asteroids grouped upon one graphic. The total number of the asteroids' spin vectors has been split up in a retrograde and a prograde part, compared with the sun's spin. The left graphic shows the retrograde part and the right part the prograde. The ecliptic latitudes, which are the asteroids' individual spin latitudes above (positive) or below (negative) the individual asteroids' orbital plane, are given by Sin β_o

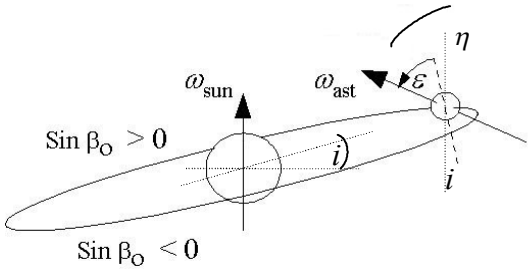

Fig. 2.2 : definition of the ecliptic latitude Sin β_O of the asteroid's spin vector : β_O is positive above the orbital plane. Definition of prograde and retrograde spin vector. The spin is prograde if its sense is directed above the orbital plane, and is retrograde if its spin sense is directed below its orbital plane.

In fig. 2.2 we find the definition of ecliptic latitude Sin β_o of the asteroid's spin vector : β_o is positive above the orbital plane. The definition of a prograde and a retrograde spin vector is given as well. The spin is prograde if its sense is directed above the orbital plane, and is retrograde if its spin sense is directed below its orbital plane.
We have to pay attention with making conclusions from the fig. 2.1, because the orbital inclinations are divided in only two groups, and the spin vector obliquities are not precisely related to these orbital inclinations. Nevertheless, we can find several results.
A first discovery is the presence of nearly 64% prograde asteroids versus 36% retrograde asteroids.
The second is that in the prograde part, the majority of the asteroids (a quantity of 30) shows an average orbital inclination of less than 10% , against a quantity of 18 with an average orbital inclination of more than 10%. In the retrograde part, we find 11 asteroids with orbital inclination of less than 10%, against 14 asteroids that have an average orbital inclination of more than 10%.
Thirdly, there are almost no spin vectors oriented in the vicinity of their own orbital plane (for Sin $\beta_o = 0$), especially in the case of orbits with a higher inclination.

2.2. Observational conclusions.

Out of this study, a number of qualitative conclusions is made. These conclusion are:

- Out of fig. 2.1 it appears that there is a significant majority of asteroids with a prograde spin vector compared to retrograde ones.
- It has been found [1] [14] that there is an absence of asteroids with their spin vector pointing in the vicinity of their orbital plane. Also the fig. 2.1 shows this.

3. The Maxwell Analogy for gravitation: equations and symbols.

The Maxwell Analogy for gravitation is the closest theory to the General Relativity of Einstein, while the universe remains Euclid and is not curved. The double aspect of the gravitational field is expressed by the Newtonian gravitation field, supplemented with the *gravitomagnetic* field that I call *gyrotation*. This latter field has been proposed by Oliver Heaviside at the end of the 19th century. The so-called Gyro-gravitation Theory, which is this very same theory, but including a new physical definition for 'the observer'[2], is suitable to explain celestial mechanics for steady and quasi-steady systems. The retardation of gravitation due to its finite velocity is not taken in account and this does not affect the results noticeably.
For the basics of the theory, I refer the reader to my paper: "*Analytic Description of Cosmic Phenomena Using the Heaviside Field*"[2]. The most relevant parts are summarized in the next paragraphs.

3.1. The general equations of the Maxwell Analogy for gravitation.

The gyro-gravitation laws can be expressed in equations (3.1) up to (3.6) below.
The electric charge is then substituted by mass, the magnetic field by gyrotation, and the respective constants are also substituted. The gravitation acceleration is written as $\boldsymbol{g}$, the so-called *gyrotation field* as $\boldsymbol{\Omega}$, and the universal gravitation constant out of $G^{-1} = 4\pi\zeta$, where G is the universal gravitation constant. We use the sign $\Leftarrow$ instead of $=$ because the right-hand side of the equations causes the left-hand side. This sign $\Leftarrow$ will be used when we want insist on the induction property in the equation. F is the resulting force, v the relative velocity of the mass m with density ρ in the gravitational field. And $\boldsymbol{j}$ is the mass flow through a fictitious surface. Bold fonts represent vectors.

$$\boldsymbol{F} \Leftarrow m\,(\boldsymbol{g} + \boldsymbol{v} \times \boldsymbol{\Omega}) \qquad (3.1)$$

$$\nabla \cdot \boldsymbol{g} \Leftarrow \rho / \zeta \qquad (3.2)$$

$$c^2\,\nabla \times \boldsymbol{\Omega} \Leftarrow \boldsymbol{j} / \zeta + \partial \boldsymbol{g} / \partial t \qquad (3.3)$$

$$div\,\boldsymbol{j} \Leftarrow -\,\partial\rho / \partial t \qquad (3.4)$$

$$div\,\boldsymbol{\Omega} \equiv \nabla \cdot \boldsymbol{\Omega} = 0 \qquad (3.5)$$

$$\nabla \times \boldsymbol{g} \Leftarrow -\,\partial \boldsymbol{\Omega} / \partial t \qquad (3.6)$$

It is possible to speak of gyro-gravitation waves with transmission speed c.

$$c^2 = 1 / (\zeta\,\tau) \qquad (3.7) \qquad \text{wherein} \qquad \tau = 4\pi\,G/c^2.$$

3.2. Calculation of the gyrotation of a spinning sphere.

For a spinning sphere with rotation velocity ω, the result for gyrotation outside the sphere is given by the vector equation (3.8) . In fig. 3.1, one equipotential line of the gyrotation vector $\boldsymbol{\Omega}$ has been traced for a spinning sphere with radius R , a moment of inertia I and a spinning velocity vector $\boldsymbol{\omega}$ at a distance vector $\boldsymbol{r}$ from the sphere's centre.

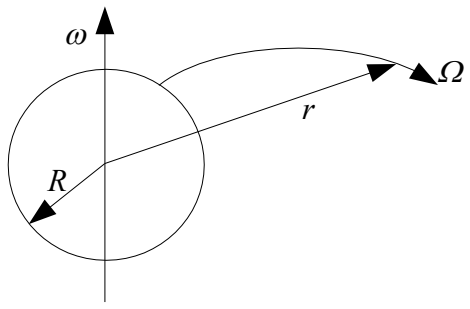

Fig. 3.1 : A spinning sphere with radius R and rotation velocity $\boldsymbol{\omega}$ is generating a rotary gravitation field (or "gyrotation" field) $\boldsymbol{\Omega}$ at a distance $\boldsymbol{r}$ from the sphere's centre.

$$\Omega_{ext} \Leftarrow \frac{G\,I}{2\,r^3\,c^2}\left(\omega - \frac{3\,r\,(\omega \bullet r)}{r^2}\right) \qquad \text{wherein for a sphere :} \qquad I = \frac{2}{5}\,m\,R^2 \qquad (3.8.a)\ (3.8.b)$$

The value of the gyrotation can be found at each place in the universe, and is decreasing with the third power of the distance r . The factor $\boldsymbol{\omega} \bullet \boldsymbol{r}$ represents the scalar vector-product, and this value is zero at the equatorial level.

In fig. 3.2 , the definition of the angles α and i is shown. The orbital plane of the asteroid is defined by the orbital inclination i in relation to the axis X . The exact location of the asteroid inside the orbit is defined by the angle α . The equipotential line of the gyrotation Ω through the asteroid has been shown as well. Is is clear that the gyrotation of the sun is axis-symmetric about the Z-axis.

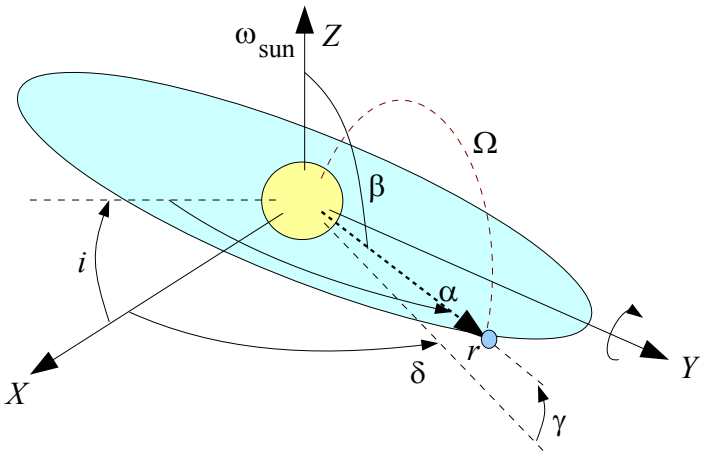

Fig. 3.2 : Definition of the angles α and i . The orbital plane is defined by the orbital inclination i in relation to the axis X . The location of the asteroid inside the orbit is defined by the angle α . The equipotential line of the gyrotation $\boldsymbol{\Omega}$ through the asteroid has been shown as well.

Now, we need to write the equation (3.8) in full for each of the components, in the case of the solar sphere.

Therefore, we need to know the angle β in terms of the inclination i and the position angle α , since the scalar vector-product of (3.8 a) is defined by $\omega\, r \cos\beta$.

Therefore we notice that (see fig.3.2): $$r \sin\gamma = r_z = r \cos\alpha \sin i \qquad (3.8.c)$$

And since $\sin\gamma = \cos\beta$, we get : $$\cos\beta = \cos\alpha \sin i \qquad (3.8.d)\ (3.8.e)$$

Hence,

$$\left(\Omega_x, \Omega_y, \Omega_z\right) = \frac{G\, m\, R^2}{5 r^3 c^2}\left[\left(0, 0, \omega_z\right) - \frac{3}{r^2}\left(r_x, r_y, r_z\right)\left(\omega\, r \cos\alpha \sin i\right)\right] \qquad (3.9)$$

wherein $$\left(r_x, r_y, r_z\right) = r\left(\cos\alpha \cos i, \sin\alpha, \cos\alpha \sin i\right) \qquad (3.10)$$

The equations (3.9) and (3.10) constitute the detailed vector formula of the equation (3.8). Remark that $\omega_Z = \omega = \omega_{sun}$. In the next chapters we will analyze the torque which is exerted by the gyrotational part of the gyro-gravitation.

Firstly, we have to analyse the effects of gyrotation on the asteroid. Some of the components of the gyrotation will affect the spin or the motion of the asteroid, other components will not affect the asteroid's motion.

For the calculation of the torque on the asteroid, we need a few mathematical steps. In the first place, we have to find the relationship between the sun's coordinate system and the most simple possible coordinate system of the asteroid. When we have this mathematical relationship, the torque can be analysed and the conditions for a maximum torque can be found in relation to the orbital inclination of the asteroid and to the obliquity of the spin vector.
Let us first express the gyrotation field in the asteroid's local coordinates.

3.3. Coordinate system transformations.

In this chapter, we will study the general implications of the gyrotational field on the asteroid.

We define the axial tilt η as : $$\eta = \varepsilon + i \qquad (3.11)$$

whereby the angle of axial tilt η, the obliquity angle ε and the angle of orbital inclination i are chosen in the same plane. The axial tilt or spin vector tilt is the tilt of the asteroid compared with the Sun's reference spin vector.

The asteroid spins with an angular velocity $\boldsymbol{\omega}_{\text{ast}}$ around the Z''-axis. The coordinate system $X'\ Y'\ Z'$ is the translated solar coordinate system $X\ Y\ Z$ over the distance of the asteroid's orbital radius r and an angle α in the orbital plane that is inclined with angle i.
We do not consider orbital eccentricity in this paper.

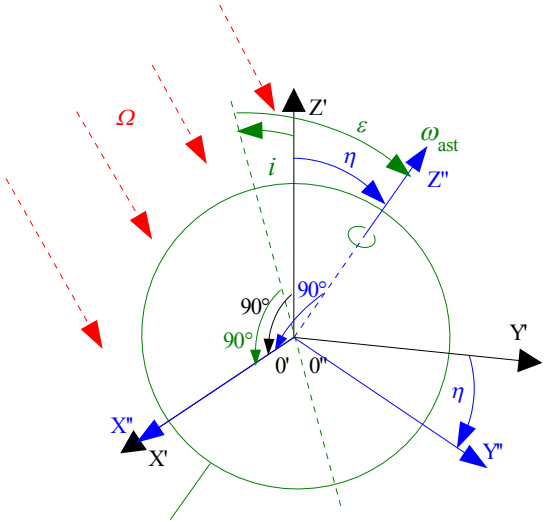

Fig. 3.3. : coordinate system transformation. The asteroid spins with an angular velocity $\boldsymbol{\omega}_{\text{ast}}$. The coordinate system $X'\ Y'\ Z'$ is the translated solar coordinate system $X\ Y\ Z$ over the asteroid's orbital radius r and an angle α in the orbital plane that is inclined with angle i. The spin axis of the asteroid is defined by the angle η, which is the axial tilt of the spin vector. The X and Y axes of the solar coordinate system are chosen such that the coordinate system $X''\ Y''\ Z''$ is a rotated coordinate system $X'\ Y'\ Z'$ over the angle η while the axis X' remains identical to X''. The orbital inclination i is shown here in the same plane as $Z\,Z'$.

The spin axis of the asteroid is defined by the angle η, which is the axial tilt of the spin vector. The X and Y axes of the solar coordinate system are chosen such that the coordinate system $X''\ Y''\ Z''$ is a rotated coordinate system $X'\ Y'\ Z'$ over the angle η while the axis X' remains identical to X''. The orbital inclination i is shown here in the same plane as $Z\,Z'$ and as η. We have represented the sun's gyrotation field, which has to be considered uniform in the case of asteroids because of their small sizes.

It is clear that the asteroid's axial tilt η is not totally defined in space here, because any tilt orientation upon the cone's surface with symmetry axis Z' and angle η will comply with the description. However, the role that the exact tilt definition would play is very small, since each place upon the cone will be described once at each orbital revolution. The lack of exact tilt coordinates could play a role for large orbital inclinations, but not for smaller inclinations. Exact tilt coordinates could be preferred for a detailed study of individual asteroids, which is not the aim of this paper.

Based on fig. 3.3 in the former chapter, we can write down the related equations between the coordinate system $X''\ Y''\ Z''$ and $X'\ Y'\ Z'$.

The relationships between both coordinate systems are given by :

$$(X'',Y'',Z'') = (X',Y'\cos\eta + Z'\sin\eta, -Y'\sin\eta + Z'\cos\eta) \qquad (3.12.a)$$

and inversely :

$$(X',Y',Z') = (X'',Y''\cos\eta - Z''\sin\eta, Y''\sin\eta + Z''\cos\eta) \qquad (3.12.b)$$

The study will be continued in the coordinate system $X''\ Y''\ Z''$.
When we want to calculate the torque of the sun's gyrotation onto the asteroid, we will have to rotate the initial gyrotation from the coordinate system $X'\ Y'\ Z'$ to the coordinate system $X''\ Y''\ Z''$.

Hence, $$\left(\Omega''_x, \Omega''_y, \Omega''_z\right) = \left(\Omega_x, \Omega_y \cos\eta + \Omega_z \sin\eta, -\Omega_y \sin\eta + \Omega_z \cos\eta\right) \quad (3.13)$$

Now we know the values of the gyrotation on the asteroid in the coordinate system $X''\ Y''\ Z''$ and are now ready to calculate the angular acceleration due to this field onto the asteroid.

3.4. The angular acceleration and the torque of the solar gyrotation acting onto an asteroid.

In fig. 3.4 we consider an asteroid under the influence of the solar gyrotation Ω''.

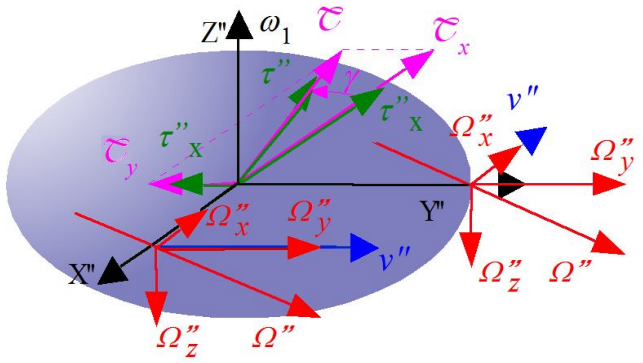

Fig. 3.4 : we consider the asteroid under the influence of the gyrotation Ω''. The asteroid is rigid, and the only motion-related acceleration is a''_z.

Two cases are shown: a velocity that is perpendicular to the X'' axis and one that is perpendicular to the Y'' axis. The gyrotation Ω'' has been split up in its components (Ω''_x, Ω''_y, Ω''_z).

When applying the equation (3.1) for each of the components, we get the forces that works onto the asteroid due to gyro-gravitation. Let us firstly write this result as an acceleration only, and omit the gravitational part, because it does not play any role for the torque of the asteroid.
Hence,

$$\left(a''_x, a''_y, a''_z\right) = \left(v''_y\ \Omega''_z, v''_x\ \Omega''_z, v''_x\ \Omega''_y - v''_y\ \Omega''_x\right) \quad (3.14.a)$$

But the asteroid is rigid, and some accelerations will have no other effect but internal compression of the matter, and the stability of the asteroid. When a''_x or a''_y, or both, are directed towards the asteroid's centre, we get an unstable asteroid. If both a''_x and a''_y are directed outwards, we get a stable asteroid. The study of the asteroid's stability is made in Appendix A.
The motion-related accelerations are : $$\left(a''_x, a''_y, a''_z\right) = \left(0, 0, v''_x\ \Omega''_y - v''_y\ \Omega''_x\right) \quad (3.14.b)$$

Only the component which is perpendicular to the asteroid's equator is relevant for the torque. In other words, Ω''_z is not relevant for it.
This means that locally, the following gyrotational equations can be written down (see fig. 3.4).

$$a''_{z(y)} = v''_x \Omega''_y \quad \text{and} \quad a''_{z(x)} = v''_y \Omega''_x \quad (3.15.a)\ (3.15.b)$$

However, if we want to describe the totality of the angular acceleration τ'' on the asteroid, we should re-write (3.1) for angular motions. The purely Newtonian gravitational part is omitted in (3.16) and (3.17).

$$\tau''_x = \omega_1 \Omega''_y \quad \text{and} \quad \tau''_y = \omega_1 \Omega''_x \quad (3.16)\ (3.17)$$

For the torque $\mathcal{T}$, we get :

$$\mathcal{T}_x = I_1 \omega_1 \Omega''_y \quad \text{and} \quad \mathcal{T}_y = I_1 \omega_1 \Omega''_x \quad (3.18)\ (3.19)$$

Remark that $\mathcal{T}_z = 0$.

The equations (3.18) and (3.19) can be written in full by using the equation (3.9) , (3.10) and (3.13). So we get:

$$\boxed{\mathcal{T}_x = \frac{G\,m\,R^2\,\omega\,I_1\,\omega_1}{5\,r^3\,c^2}\left(\left(1-\frac{3}{4}\sin^2 2\alpha\right)\sin\eta - \frac{3}{2}\sin 2\alpha\,\sin i\,\cos\eta\right)} \qquad (3.20)$$

$$\boxed{\mathcal{T}_y = -\frac{3\,G\,m\,R^2\,\omega\,I_1\,\omega_1}{10\,r^3\,c^2}\cos^2\alpha\,\sin 2i} \qquad (3.21)$$

The equations (3.20) and (3.21) define the solar gyrotational torques on asteroids for each orbital inclination, but also on each location on the orbit.

4. Conditions for a maximal and minimal gyrotation on the asteroid's orbital inclination.

4.1. Forced gyroscopic motion.

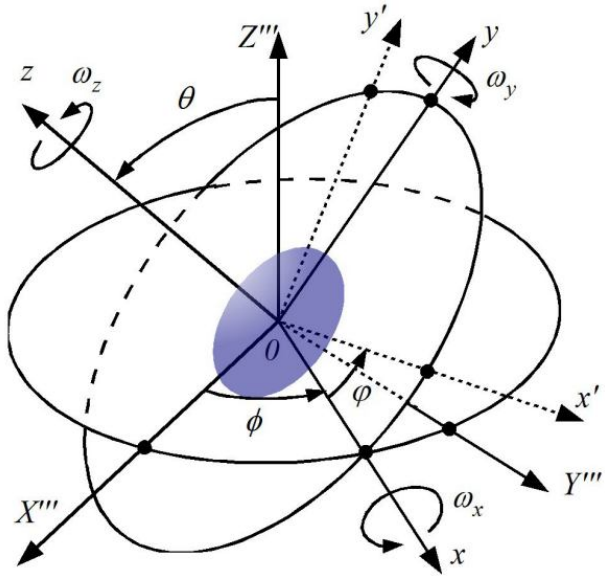

Fig. 4.1 : Precession and nutation of an asteroid.

Let us consider the forced gyroscopic motion upon the asteroid. The spin axis of the asteroid is the Z''' -axis.

We define the following notations for the Euler angles : the precession angle ϕ , the nutation angle θ and the spin angle φ of the asteroid.

In the coordinate system $x\,y\,z$, the angles θ and ϕ are needed to define a location.
In the coordinate system $x'y'z'$, the angles θ , ϕ and φ are needed to define a location.

In the respective coordinate systems, the following relationships are valid.
The angular velocity ω in $x'y'z'$ is given by :

$$\omega_x = \dot{\theta} \qquad (4.1)$$

$$\omega_y = \dot{\phi}\sin\theta \qquad (4.2)$$

$$\omega_z = \dot{\phi}\cos\theta + \dot{\varphi} \qquad (4.3)$$

The angular velocity ψ in $x\,y\,z$ is given by :

$$\psi_x = \dot{\theta} \qquad (4.4)$$

$$\psi_y = \dot{\phi}\sin\theta \qquad (4.5)$$

$$\psi_z = \dot{\phi}\cos\theta \qquad (4.6)$$

The angular momenta are :

$$L_x = I_x\,\omega_x = I_0\,\dot{\theta} \qquad (4.7)$$

$$L_y = I_y\,\omega_y = I_0\,\dot{\phi}\sin\theta \qquad (4.8)$$

$$L_z = I_z\,\omega_z = I_1\left(\dot{\phi}\cos\theta + \dot{\varphi}\right) \qquad (4.9)$$

wherein we define a cylinder-symmetric asteroid with the inertia momenta : $I_0 = I_x = I_y$ and $I_1 = I_z$, and wherein $\dot{\theta}$, $\dot{\phi}$ and $\dot{\varphi}$ are time-derivatives of θ , ϕ and φ .

The equations of motion are then :

$$\dot{L}_x - L_y\psi_z + L_z\psi_y = \mathcal{T}_x \qquad (4.10)$$

$$\dot{L}_y - L_z\psi_x + L_x\psi_z = \mathcal{T}_y \qquad (4.11)$$

$$\dot{L}_z - L_x\psi_y + L_y\psi_x = \mathcal{T}_z \qquad (4.12)$$

wherein ***L*** is the angular momentum and $\mathcal{T}$ is the solar gyrotation torque that works upon the asteroid.
Notice that in this paper $\dot{\varphi} \equiv \omega_1$, where ω_1 is the spinning velocity of the asteroid.

Remark that the orientation of the coordinate system $X'''\,Y'''\,Z'''$ is not defined yet. We chose it such that the Z'''-axis corresponds with the Z'' axis, and the X'''-axis corresponds with the torque defined as $\mathcal{T}_{xy} \equiv \sqrt{\mathcal{T}_x^2 + \mathcal{T}_y^2}$ and its orientation (angle γ in the coordinate system $X'''\,Y'''\,Z'''$) given by $\tan\gamma = \mathcal{T}_y / \mathcal{T}_x$.

The equations of motion become, written in full :

$$I_0\left(\ddot{\theta} - \dot{\phi}^2 \sin\theta\cos\theta\right) + I\ \dot{\phi}\sin\theta\left(\dot{\phi}\cos\theta + \dot{\varphi}\right) = \mathcal{T}_{xy} \tag{4.13}$$

$$I_0\left(\ddot{\phi}\sin\theta + 2\,\dot{\phi}\dot{\theta}\cos\theta\right) - I\ \dot{\theta}\left(\dot{\phi}\cos\theta + \dot{\varphi}\right) = 0 \tag{4.14}$$

$$I\left(\ddot{\varphi} + \ddot{\phi}\cos\theta - \dot{\phi}\dot{\theta}\sin\theta\right) = 0 \tag{4.15}$$

Due to the high number of solutions, we should simplify these equations by setting a minimum of restrictions.

Suppose that $\ddot{\varphi} = 0$, or, in other words, the spinning velocity can be seen as a constant.

Out of (4.15) and (4.14) we find for the precession velocity : $$\dot{\phi} \approx \frac{I\ \omega_1}{\left(2I_0 - I\right)\cos\theta} \tag{4.16}$$

The calculation is summarized in Appendix B. Since θ is not known yet, we can get it from (4.13) by using (4.16).

We know that by definition, the nutation and the change of tilt position are equal, thus : $\theta = \Delta\eta$.

For the angle $\Delta\eta$ we find (see Appendix B) : $$\boxed{\Delta\eta = \arctan\left(\mathcal{T}_{xy}\,\frac{\left(2I_0 - I\right)^2}{I_0 I^2 \omega_1^2}\right)} \tag{4.17}$$

The value of the nutation is however not constant. The angular velocity of the nutation, $\dot{\theta}$, can be found by differentiating (4.17) to the time.

Knowing that $\mathrm{d}\theta/\mathrm{d}t = \omega_0\,\mathrm{d}\theta/\mathrm{d}\alpha$, wherein ω_0 is the orbital velocity of the asteroid, we get (see Appendix B):

$$\dot{\theta} = \omega_0\frac{\mathrm{d}\theta}{\mathrm{d}\alpha} = \omega_0\frac{\left(2I_0 - I\right)^2}{I_0 I^2\omega_1^2}\frac{\mathrm{d}\mathcal{T}_{xy}}{\mathrm{d}\alpha} \tag{4.18}$$

The vector $\mathcal{T}_{xy}$ is rotating about the Sun, together with the asteroid's orbit. It fluctuates between a certain minimal value and its maximal value, due to the oscillations of α .

4.2. Calculation of the spin vector tilt changes.

The calculation of the spin vector tilt changes can be realized by using (4.17), worked out with the equations (C.2) to (C.6) of appendix C.

The change of the tilt occurs continuously by the equation (C.6).

$$\boxed{\Delta\eta \approx \frac{G\,m\,R^2\,\omega}{5\,r^3 c^2}\,\frac{\left(2I_0 - I\right)^2}{I_0\,I\,\omega_1}\left(2 + \frac{9}{8}\,\frac{\sin^2 2i}{\sin^2\eta}\right)\sin\eta} \qquad \text{(C.6)}$$

After every orbital semicircle, the tilt change with a very tiny portion. It will swing back during the next orbital semicircle.

4.3. Calculation of the precession changes.

The precession velocity of equation (4.16) can further be simplified to:

$$\boxed{\dot{\phi} = \frac{I\,\omega_1}{2I_0 - I}} \qquad (4.19)$$

because of the very small values of θ.

5. Discussion and conclusions.

Based on our theoretical results, we come to a certain number of confirmations of the observed data by E. Skoglöv and A. Erikson. Let us take the points one by one and comment it. The equations (3.20) and (3.21), (C.6), and fig.A.1 are the main theoretical data whereon the correlation can be tested.

– the heliocentric distance is relevant for the spin vector behaviour.

This property follows directly from (3.20) and (3.21). The dependency from the distance to the sun is inverse, with an exponent 3.

– the spin tilt oscillations' amplitude increases with the increasing orbital inclination of the asteroid.

The main theoretical data, see equation (C.6), confirm the increasing values of the oscillations with increasing orbital inclination *i* and, consequently, of its torque and its precession.

– the largest spin oscillations' amplitudes are found if the initial spin vector lays in the orbital plane.

At an axial tilt of $\eta = \pi/2$, the acceleration's values are the largest, according to the main theoretical data. Since the values η and ε are relatively similar for values around $\eta = \pi/2$ and for not too important orbital inclinations, there is a good correlation between the observed and the theoretical data.

– the spin obliquity differences are generally insensitive to the shape, composition and spin rate of the asteroids.

This is not what we found theoretically. It is not clear why the observational data do not discover this, but probably the reason is that the high impact of the orbital inclination totally masks the observational data of the other influencing parameters.

We found a flaw in the representativity of the graphical concepts of E. Skoglöv and A. Erikson, especially for the fig.1.2 and fig. 1.3. To show this, let us define $\varepsilon = \arctan(X_0) - i$, so that $\eta = \varepsilon + i = \arctan(X_0)$, and the function $X = \cos(\arctan(X_0) - i)$, which is only a transcription of the definition $X = \cos\varepsilon$, apart from the term $-i$. This function only depends from the orbital inclination *i* and from the initial, fixed $\cos\varepsilon_0$. Now we found that the shape of curve that this function represents, is virtually the same as the one of fig.1.2. In other words, the only fact of the inclusion of the orbital inclination *i* already gives the curve shapes of fig.1.2, totally independently from any observations. The supposed (strong) dependence of the orbit inclination to the spin vector tilt η is namely only fictive in that graphic. The same is valid for the function represented by function $\Delta X = \cos(\arctan(X_0) - i) - X_0$ compared with fig.1.3, which supposes a strong dependency from the spin vector obliquity ε that however is almost only caused by the part of the orbital inclination *i*. The influence of other parameters appear to be severely masked as well in these graphics. In other words, the choice of associating the tilt with the obliquity angle ε is unfortunate for observational data, because the real tilt η is totally masked by the influence of the inclination *i*. It would be likely to get the observational data in the form $\Delta\eta = f(\eta, i)$.

– the spin vectors of prograde asteroids are more chaotic than the spin vectors of retrograde asteroids.

From fig.A.1 it is clear that the stability of the asteroids theoretically comply with these findings. For prograde orbits and for large orbital inclinations, the graph shows a very strong tilt instability, while for retrograde orbits, the graph has a milder instability. However, for prograde orbits and for small orbital inclinations, the tilt instability is very low. Remark that the use of the terms 'prograde' and 'retrograde' in the theoretical part is to be related to the solar spin as a reference, while in the papers of E. Skoglöv and A. Erikson, this means : related to the reference of the ecliptic latitude. For small inclinations, the observational difference is barely noticeable.

– there is a significant majority of asteroids with a prograde spin tilt vector ($0 < \eta < \pi/2$) compared to retrograde ones ($\pi/2 < \eta < \pi$).

This property can explained by the theory, since fig.A.1 is asymmetric to the prograde and the retrograde orbits. Indeed, the prograde tilts are fully stable for small prograde orbit inclinations. Since there are more prograde orbiting asteroids, the number of prograde tilts must be higher as well.

– there is an absence of asteroids with their spin vector pointing in the vicinity of their orbital plane.

This follows from the equation (C.6) where the largest deviation of the tilt is obtained if $\eta = \pi/2$. It also follows from fig.A.1, where most of the orbit is unstable if $\eta = \pi/2$.

6. References and bibliography.

1. Barucci, M. A., D. Bockelee-Morvan, A. Brahic, S. Clairemidi, J. Lecacheux, and F. Roques 1986. Asteroid spin axes: Two additional pole determinations and theoretical implications. *Astron. Astrophys. 163,261–268.*
2. De Mees, T., 2005, Analytic Description of Cosmic Phenomena Using the Heaviside Field, *Physics Essays, Vol. 18, Nr 3.*
3. Einstein, A., 1916, Über die spezielle und die allgemeine Relativitätstheorie.
4. Erikson, A. 1999, The spin vector distribution of main belt asteroids. *Bull. Am. Astron. Soc. 31,1112.*
5. Erikson, A. 2000. The present distribution of asteroid spin vectors and its relevance to the origin and evolution of main belt asteroids. *DLR-Forschungsbericht 2000—37. DLR,Köln.*
6. Feynman, Leighton, Sands, 1963, Feynman Lectures on Physics *Vol 2.*
7. Heaviside, O., A gravitational and electromagnetic Analogy, *Part I, The Electrician, 31, 281-282 (1893)*
8. Jefimenko, O., 1991, Causality, Electromagnetic Induction, and Gravitation, *Electret Scientific, 2000.*
9. Laskar, J., and P. Robutel, 1993, The chaotic obliquity of the planets, *Nature 361, 608–612.*
10. Skoglöv, E. 1999, Spin vector evolution for inner solar system asteroids. *Planet. Space Sci. 47,11–22.*
11. Skoglöv, E., P.Magnusson, and M. Dahlgren, 1996. Evolution of the obliquities for ten asteroids. *Planet. Space Sci. 44,1177–1183.*
12. Skoglöv, E., 2001, The Influence of the Orbital Evolution of Main Belt Asteroids, *Icarus 160.*
13. D. Vokrouhlický, D. Nesvorný, 2006, W.F. Bottke, Secular spin dynamics of inner main-belt asteroids*, Icarus 184.*
14. Zappalà, V., and Z. Knevžević 1984. Rotation axes of asteroids: Results for 14 objects, *Icarus 59,435–455.*

Appendix A : Tilt stability study of the asteroids.

From (3.15) it follows that the larger a''_z is, the more instable the asteroid's tilt. With (3.20) we see that the most instable situation occurs if, roughly speaking, $\eta = \pi / 2$.

But a''_z is not the only factor for stability.

A stable asteroid's tilt is also given by the condition $a''_x > 0$ or $a''_y > 0$. A labile asteroid is obtained if $a''_x < 0$ or $a''_y < 0$. We have indifference if $a''_x = 0$ or $a''_y = 0$. With (3.14.a) and with the angular notation such as in (3.16) and (3.17), we conclude that tilt stability indifference occurs if $\Omega''_z = 0$.

When using (3.9), (3.10) and (3.13), we come to the following conditions for an indifference of the tilt stability :

$$\tan\eta = \frac{3\cos^2\alpha\ \sin^2 i - 1}{3\sin\alpha\ \cos\alpha\ \sin i} \qquad \text{(A.1)}$$

Graphically, the equation (A.1) has been plotted in fig. A.1.

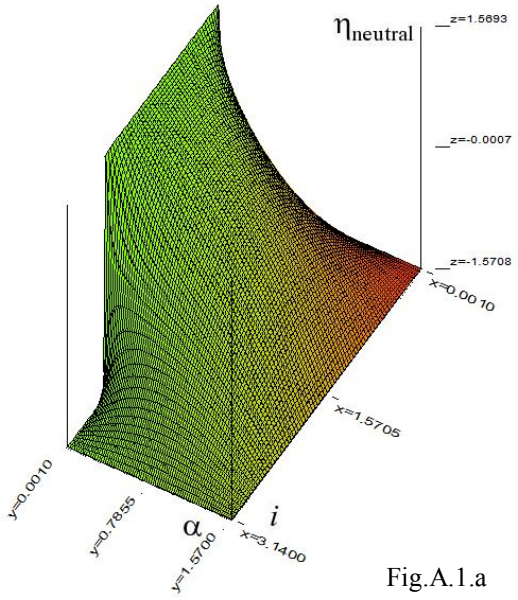

Fig.A.1.a

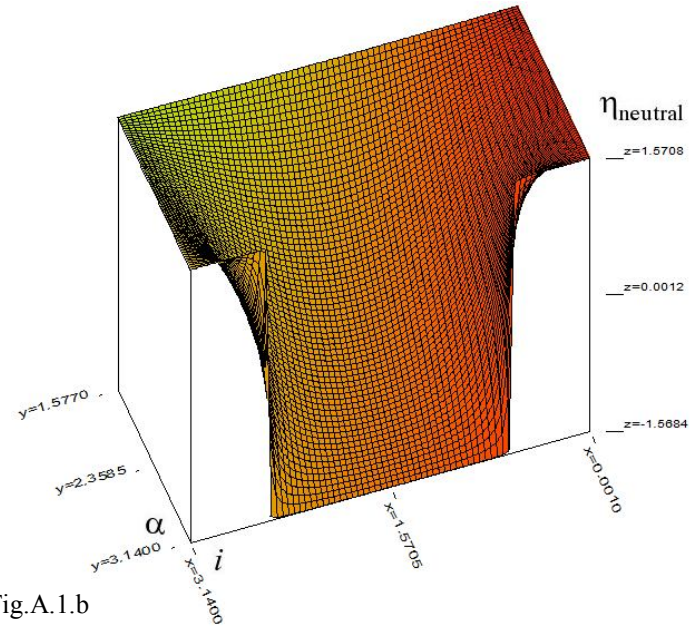

Fig.A.1.b

Fig. A.1.a and b.: Plot of the neutral tilt angle $\eta_{neutral}$ in relation to the angular location α and the orbital inclination i. Values of η that are higher than $\eta_{neutral}$ (northern semicircle) or lower (southern semicircle) will give a stable asteroid's tilt. Values of η that are lower than $\eta_{neutral}$ (northern semicircle) or higher (southern semicircle) will give a unstable asteroid's tilt. Prograde orbits with small inclinations provide very stable tilts, but above an orbit inclination of about $\pi/8$, the tilts suddenly become very unstable until about $7\pi/8$, after which they become stable again for about $0 < \alpha < \pi/8$ and $7\pi/8 < \alpha < \pi$. Note that the orientation of the tilt in space has only been defined regarding the z-axis, not the x and y axes. The results for the x and y axes are averaged. However, during one orbital rotation, all the possible orientations to the x and y axes are reached.

Tilt stability is obtained if $\Omega''_z > 0$ or $\tan\eta > \left(3\cos^2\alpha\ \sin^2 i - 1\right) \Big/ \left(3\sin\alpha\ \cos\alpha\ \sin i\right)$ and this occurs if $\eta > \eta_{neutral}$ (northern semicircle) or $\eta < \eta_{neutral}$ (southern semicircle); unstable tilt is obtained if $\Omega''_z < 0$ or $\tan\eta < \left(3\cos^2\alpha\ \sin^2 i - 1\right) \Big/ \left(3\sin\alpha\ \cos\alpha\ \sin i\right)$ and this occurs if $\eta > \eta_{neutral}$ (southern semicircle) or

$\eta < \eta_{\text{neutral}}$ (northern semicircle). For fig. A.1, this means that the zone between both neutral curves is unstable, but that the zone outside is stable. Roughly speaking, we conclude out of fig. A.1 , that when the orbit inclination is smaller than nearly $\pi/8$, as well prograde as retrograde, the tilt is highly stable. However, once the orbit inclination is higher than $\pi/8$, there is a sudden switch to an unstable tilt. Then, the tilt will swing northwards or southwards, depending from the position at that time in the northern or the southern orbit semicircle.
Remark that the zone of tilt stability is much wider in α for prograde orbits if $0 < i < \pi/8$ then for retrograde orbits when $7\pi/8 < i < \pi$.
This the main reason why the planet's tilt in our solar system are stable. Venus' tilt, which is opposite, might have been originated because of an original orbit inclination wherefore $i > \pi/8$, causing a tilt instability and even a tilt switch, without any collision with other bodies. As known by former papers, the inclined orbits tend to swivel into prograde orbits that are nearly in the Sun's equatorial plane.

Note that the orientation of the tilt in space has only been defined regarding the *z*-axis, not against the *x* and *y* axes. The results for the *x* and *y* axes are averaged. However, during one orbital rotation, all the possible orientations to the *x* and *y* axes are reached.

Appendix B : Calculation of the precession and the nutation.

Since $\ddot{\varphi} = 0$, from (4.15) we get : $\ddot{\phi} = \dot{\phi}\,\dot{\theta}\tan\theta$.

Using this in (4.14) gives : $$\dot{\phi} = \frac{I\,\dot{\varphi}}{\left(I_0\left(2+\tan^2\theta\right)-I\right)\cos\theta} \tag{B.1}$$

Wherein $\tan^2\theta << 2$.

We can use (B.1) in (4.13) and we obtain : $$\dot{\varphi}^2\,\frac{I^2 I_0}{\left(2I_0 - I\right)^2}\tan\theta = \mathcal{T}_{xy} \tag{B.2}$$

or for the nutation angle : $$\theta = \arctan\left(\mathcal{T}_{xy}\,\frac{\left(2I_0 - I\right)^2}{I_0 I^2 \dot{\varphi}^2}\right) \tag{B.3}$$

The nutation velocity is found as follows: since $\mathrm{d}\theta/\mathrm{d}t = \omega_0\,\mathrm{d}\theta/\mathrm{d}\alpha$, wherein ω_0 is the orbital velocity of the asteroid, we find :

$$\dot{\theta} = \omega_0\frac{\mathrm{d}\theta}{\mathrm{d}\alpha} = \omega_0\,\frac{\left(2I_0 - I\right)^2}{\left(1+\left(\frac{\mathcal{T}_{xy}\left(2I_0 - I\right)^2}{I_0 I^2\omega_1^2}\right)^2\right) I_0 I^2\omega_1^2}\,\frac{\mathrm{d}\mathcal{T}_{xy}}{\mathrm{d}\alpha} \tag{B.4}$$

which can be simplified to : $$\dot{\theta} = \omega_0\frac{\mathrm{d}\theta}{\mathrm{d}\alpha} = \omega_0\,\frac{I_0 I^2\omega_1^2\left(2I_0 - I\right)^2}{\left(I_0^2 I^4\omega_1^4 + \mathcal{T}_{xy}^2\left(2I_0 - I\right)^4\right)}\,\frac{\mathrm{d}\mathcal{T}_{xy}}{\mathrm{d}\alpha} \tag{B.5}$$

We know that $\mathcal{T}_{xy}$ is very small in this application, and hence :

$$\dot{\theta} = \omega_0\frac{\mathrm{d}\theta}{\mathrm{d}\alpha} \approx \omega_0\,\frac{\left(2I_0 - I\right)^2}{I_0 I^2\omega_1^2}\,\frac{\mathrm{d}\mathcal{T}_{xy}}{\mathrm{d}\alpha} \tag{B.6}$$

The same result as (B.6) can be found by using (B.1) in (4.13) while supposing $\ddot{\theta}$ small enough to be neglected and θ small enough to consider that $\tan\theta = \theta$. This confirms a good credibility of the parametric choices.

Let us work out (B.6). We defined $$\mathcal{C}_{xy} = \sqrt{\mathcal{C}_x^2 + \mathcal{C}_y^2} \tag{B.7}$$

Working out (B.6) will need us to find the result of $$\frac{\mathrm{d}\,\mathcal{C}_{xy}}{\mathrm{d}\,\alpha} = \frac{\mathcal{C}_x \dfrac{\mathrm{d}\,\mathcal{C}_x}{\mathrm{d}\,\alpha} + \mathcal{C}_y \dfrac{\mathrm{d}\,\mathcal{C}_y}{\mathrm{d}\,\alpha}}{\sqrt{\mathcal{C}_x^2 + \mathcal{C}_y^2}} \quad . \tag{B.8}$$

The derivatives are :

$$\frac{\mathrm{d}\,\mathcal{C}_x}{\mathrm{d}\,\alpha} = \frac{3\,G\,m\,R^2\,\omega\,I_1\,\omega_1}{5\,r^3\,c^2}\cos 2\alpha\left(\sin 2\alpha \sin\eta - \sin i\cos\eta\right) \tag{B.9}$$

and

$$\frac{\mathrm{d}\,\mathcal{C}_y}{\mathrm{d}\,\alpha} = \frac{3\,G\,m\,R^2\,\omega\,I_1\,\omega_1}{10\,r^3\,c^2}\sin 2\alpha \sin 2i \tag{B.10}$$

We do not write (B.6) in full with the results that we find in (B.9) and (B.10), but it is clear that there is a solution.

Appendix C : Detailed estimation of the relevant torques and tilt variations.

Since (B.7) is relevant for any value of α , we can choose to limit our analysis to the average values of each performed orbital revolution.

We get for the values $\alpha = 0$ or $\alpha = \pi$, and $\alpha = \pi/2$ or $\alpha = -\pi/2$ the following results :

$$\sqrt{\mathcal{C}_x^2 + \mathcal{C}_y^2}\Big|_{\alpha=\pm\pi/2} = \frac{G\,m\,R^2\,\omega\,I_1\,\omega_1}{5r^3c^2}\sin\eta \tag{C.1}$$

$$\sqrt{\mathcal{C}_x^2 + \mathcal{C}_y^2}\Big|_{\alpha=0} = \frac{G\,m\,R^2\,\omega\,I_1\,\omega_1}{5r^3c^2}\sqrt{1+\frac{9}{4}\frac{\sin^2 2i}{\sin^2\eta}}\ \sin\eta \tag{C.2}$$

And this gives as an average for the total circle:

$$\sqrt{\mathcal{C}_x^2 + \mathcal{C}_y^2}\Big|_{\alpha_{av}} = \frac{G\,m\,R^2\,\omega\,I_1\,\omega_1}{5r^3c^2}\left(1+\sqrt{1+\frac{9}{4}\frac{\sin^2 2i}{\sin^2\eta}}\right)\sin\eta \tag{C.3}$$

which can be simplified, when using $\sqrt{1+x} \approx 1 + x/2$ into :

$$\sqrt{\mathcal{C}_x^2 + \mathcal{C}_y^2}\Big|_{\alpha_{av}} \approx \frac{G\,m\,R^2\,\omega\,I_1\,\omega_1}{5r^3c^2}\left(2+\frac{9}{8}\frac{\sin^2 2i}{\sin^2\eta}\right)\sin\eta \tag{C.4}$$

Equation (4.17) can then be written as follows :

$$\Delta\eta \approx \arctan\left(\frac{G\,m\,R^2\,\omega}{5r^3c^2}\frac{\left(2I_0 - I\right)^2}{I_0\ I\ \omega_1}\left(2+\frac{9}{8}\frac{\sin^2 2i}{\sin^2\eta}\right)\sin\eta\right) \tag{C.5}$$

Since the absolute value of $\Delta\eta$ is very small, we can omit the trigonometric function and set approximatively :

$$\Delta\eta \approx \frac{G\,m\,R^2\,\omega}{5\,r^3 c^2}\frac{\left(2I_0 - I\right)^2}{I_0\;I\;\omega_1}\left(2 + \frac{9}{8}\frac{\sin^2 2i}{\sin^2\eta}\right)\sin\eta \qquad \text{(C.6)}$$

Hence, (C.6) is the nutation value after half an orbital revolution, and it will swing back during the second half an orbital revolution.
For important inclinations, and especially if they are close to $\pi/2$, the tilt variations can become up to 3,25 times that of the same asteroid if it would orbit in the sun's equator plane.
The same effect occurs with satellites that orbit about the Earth (fly-by anomaly).